A Study of Three-Dimensional, Incompressible, Turbulent Wall Jets

PASQUALE M. SFORZA* AND GARY HERBST†
Polytechnic Institute of Brooklyn, Farmingdale, N. Y.

This report presents an experimental investigation of the mean properties of turbulent, three-dimensional, incompressible air jets issuing into a quiescent air ambient from various rectangular orifices parallel to, and at the surface of, a flat plate. An analytical approach to estimate the shear stress distribution at the plate is also presented. The flowfield of a three-dimensional wall jet is found to be characterized by three distinct regions in the axis velocity decay. From the results obtained it is concluded that for three-dimensional wall jets the maximum velocity in the flow in the near field exhibits a decay rate dependent on orifice geometry, whereas far downstream of the jet exit it decays at the same rate as that in a radial wall jet flow field independent of orifice geometry. Furthermore, it is shown that the growth of the mixing layer normal to the plate is apparently independent of orifice shape while the near field spanwise growth is affected by initial geometry. Irregularities in the spanwise distribution of streamwise mean velocity attest to the strong three-dimensionality in the near field of the wall jets studied. These irregularities are manifested as local excesses, or defects, in the velocity profile. Such results indicate that the characterization of the wall jet flowfield generated by a finite slot as quasi two-dimensional may be of questionable validity.

Nomenclature

CD	= characteristic decay
C_f	= skin friction coefficient, Eq. (14)
d	= height of orifice
e	= eccentricity of orifice, d/l
l	= length of orifice
PC	= potential core
RD	= radial-type decay
Re	= Reynolds number
u	= mean velocity in X direction
v,w	= mean transverse velocity components
X	= streamwise coordinate
Y	= spanwise coordinate
Z	= normal coordinate
ξ	= transformed normal coordinate, $Z/Z_{1/2}$
η	= transformed spanwise coordinate, $Y/Y_{1/2}$
θ	= Eq. (7)
ν	= kinematic viscosity
ρ	= density
τ	= shear stress
τ_{XY}	= axial shear stress on planes normal to Y axis
τ_{XZ}	= axial shear stress on planes normal to Z axis

Subscripts

m, max	= conditions at maximum velocity point
w	= conditions at the wall
X,Y,Z	= differentiation with respect to the indicated variable
0	= conditions along the X axis
$\frac{1}{2}$	= conditions at $u/u_m = \frac{1}{2}$
2-D	= two-dimensional flow conditions

Superscripts

$\bar{(\ )}$	= $(\ )/d$ unless otherwise specified

I. Introduction

AN experimental investigation of the mean properties of turbulent, three-dimensional, incompressible jets of air issuing into a quiescent air ambient, tangent to, and at the surface of, a rigid flat plate is presented. A schematic diagram of the flowfield appears in Fig. 1. Herein such flows are termed "three-dimensional wall jets." An exploratory investigation of such a three-dimensional flowfield was presented by Viets and Sforza.[1] Their results were extended in Ref. 2, upon which this article is based.

Experimental investigations of "two-dimensional" as well as radial wall jets have been performed by Sigalla,[3] Bakke,[4] Bradshaw and Gee,[5] Poreh et al.,[6] among others.[7–12] A very useful annotated bibliography on wall jets has been prepared by Rajaratnam and Subramanya.[13]

Sigalla's[3] primary objective was the determination of the surface skin-friction distribution in a so-called "two-dimensional" wall jet, whereas Bakke's[4] study centered upon a comparison of his experimental observations with Glauert's theoretical predictions for a radial wall jet. Bradshaw and Gee[5] extensively explored both mean and turbulent properties of "two-dimensional" wall jets and presented measurements of mean velocity and turbulence intensity profiles, skin-friction coefficients, etc. A similar investigation of radial wall jets has been performed by Poreh et al.[6]

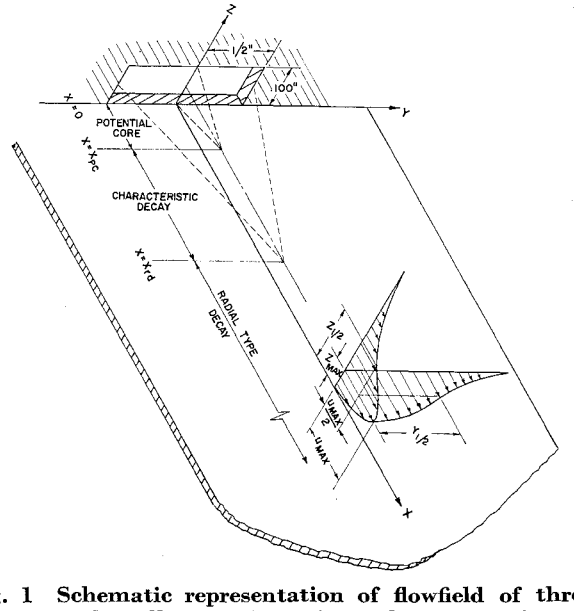

Fig. 1 Schematic representation of flowfield of three-dimensional wall jet; dimensions shown are for the orifice $e = 0.10$.

Received July 18, 1968; revision received April 18, 1969. This research was supported by the Air Force Office of Scientific Research under Contract AF 49(638)-1623, Project 9781-01.

* Associate Professor of Aerospace Engineering. Associate AIAA.

† National Science Foundation Graduate Trainee.

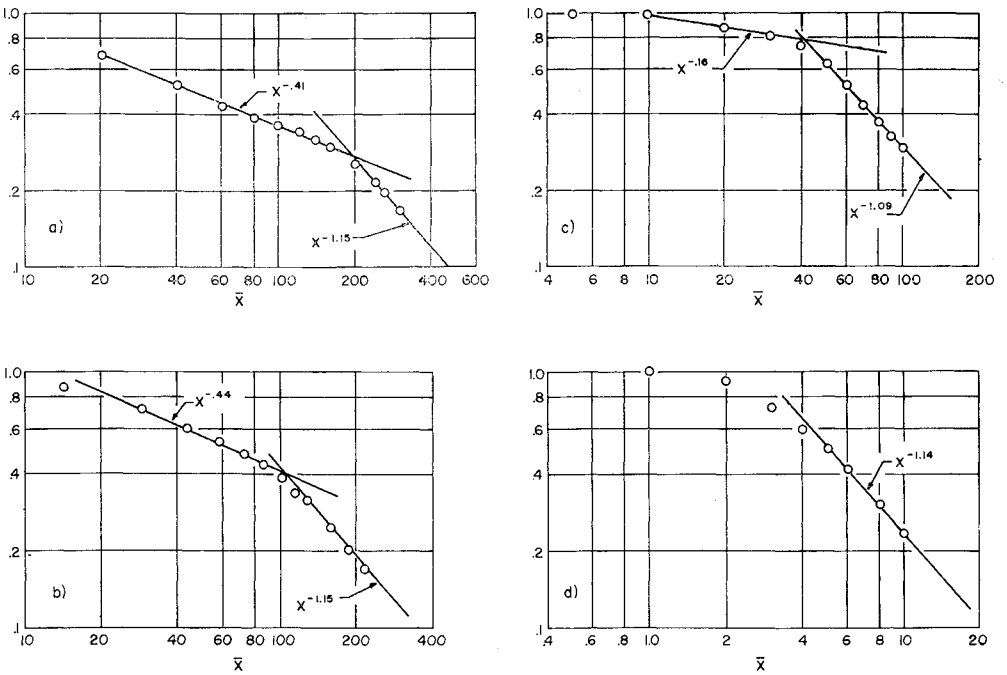

Fig. 2 Maximum velocity decay for: a) e = 0.025, b) e = 0.05, c) e = 10, d) e = 1.0.

In the present investigation the flowfields were generated by a rectangular orifice. Each orifice possessed a different eccentricity, here defined as the ratio of the height to the length of the orifice, but all orifices were of equal area. Furthermore all tests were performed with an exit velocity of 208 fps. Hence, all the flows were observed under conditions of equal initial momentum flux.

It was found that all conventional three-dimensional wall jets, i.e., those whose orifice eccentricity is less than or equal to unity, may be characterized by three distinct regions in terms of the axial decay of the maximum velocity as suggested by Viets and Sforza.[1] This feature is analogous to that encountered in the description of three-dimensional freejets as demonstrated by Sforza et al.[14] Furthermore, irregularities in the spanwise distribution of the mean streamwise velocity for the conventional three-dimensional wall jets have been observed, similar to the mean velocity irregularities in three-dimensional freejets reported by Trentacoste and Sforza.[15] These irregularities in the mean velocity profile, manifested as local excesses and defects, pose a difficulty in specifying what region of a wall jet flowfield generated by a long, slender slot is even quasi-two-dimensional. Hence the use of quotation marks about the term two-dimensional in the previous discussion. The implications of the features of wall jet flowfield will be discussed subsequently.

Finally, an estimate of the streamwise variation of the skin-friction coefficient for three-dimensional wall jets is presented. The results of the analysis, which is based on an integral form of the conventional boundary-layer equations, indicate that the streamwise variation of the skin-friction coefficient is independent of the spanwise growth of the mixing layer and is a function of the ratio of the characteristic dimension of the mixing layer (the half-width) normal to the plate to the streamwise coordinate x. The major assumption utilized in the derivation is that the spanwise surface shear stress is similar; this result is shown to be reasonable, particularly in the far field of the wall jet.

II. Experimental Apparatus

A detailed description of the wall jet facility is presented in Ref. 2. Basically, it consists of a settling chamber mounted on a rigid support which can be adjusted in the three coordinate planes. The downstream end of the settling chamber is capped by an orifice plate; each plate had an orifice of different eccentricity but an equivalent area of 0.1 in.^{2} The orifice was aligned with the surface of the highly polished 4 × 6 ft flat aluminum plate as shown in Fig. 1. This plate was also adjustable for precise alignment with the settling chamber and the traversing probe unit. The latter can be adjusted to within 0.005 in. in the Z and Y directions.

The total head and static pressure measurements were obtained by utilizing vertical (water) manometers. Pressure differentials of 0.05 in. of water were easily read with this system. Subsequent mean flow measurements with a constant current hot wire anemometer agreed very well with the Pitot probe measurements.

The pressure probes used in the present investigation are of standard design; no attempt was made to evaluate the different static probe designs considered by some to be essential to static pressure measurements in turbulent flows.

Flow visualization studies of the surface flow pattern utilizing a lamp-black and kerosene solution, and of a modelled wall jet flowfield in the PIBAL water tunnel were performed. The photographs obtained are not reported herein; they are discussed in detail in Ref. 2.

III. Presentation and Discussion of Results

General Features

It has been shown by Viets and Sforza[1] that three distinct regions may be defined for a three-dimensional wall jet (see Fig. 1). These regions are described by the different rates of decay of the maximum velocity along the centerline of the jet, and may be classified as follows:

1) Potential Core (PC) region: Here the flow is characterized by a constant maximum velocity which is equal, or very close to, the jet exit velocity.

2) Characteristic Decay (CD) region: In this second region the maximum velocity decays as a constant power of X (streamwise distance) and indicates that the mixing from the near boundaries (the top side of the orifice and the flat plate) of the jet has reached the center of the flow region, but the mixing from the far boundaries (the sides) has not yet permeated the entire flowfield. Therefore, in this region orifice end effects are important; hence the axis decay of mean velocity is termed characteristic of the particular orifice considered.

3) Radial Type (RD) Decay region: Finally, the mixing from all the boundaries of the jet has permeated the entire

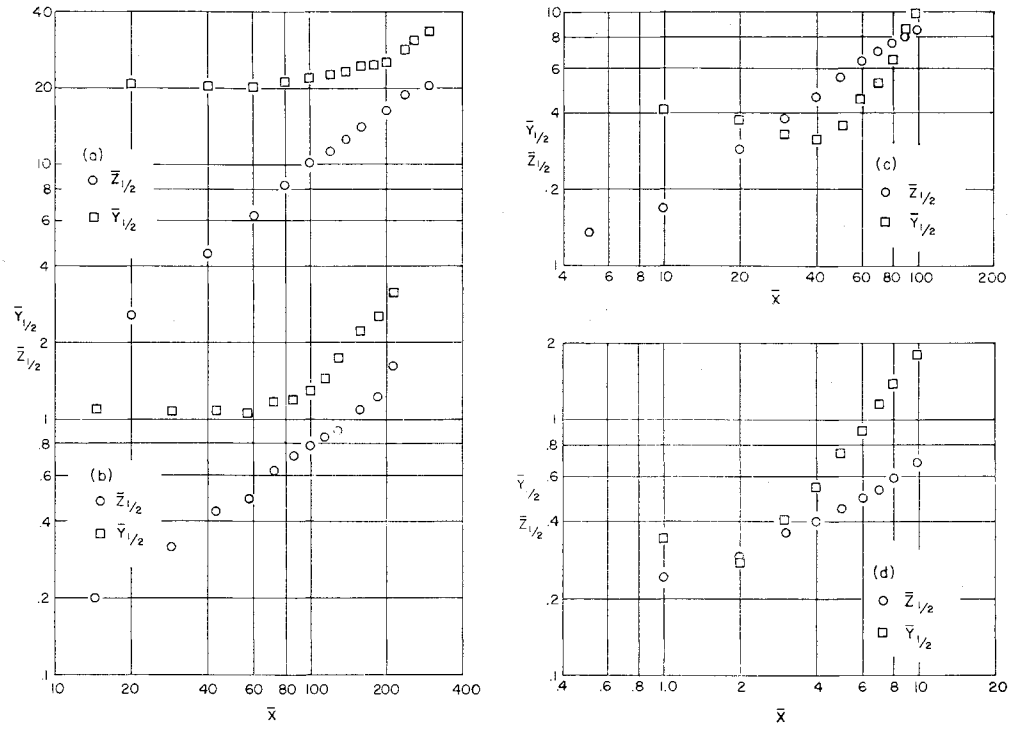

Fig. 3 Half-width growth for: a) e = 0.025, b) e = 0.05, c) e = 0.10, d) e = 1.0.

flowfield. The maximum velocity decays like that of a radial wall jet, i.e., an axisymmetric jet which impinges normally upon a wall and spreads radially over the wall. In this region the flow becomes increasingly oblivious of the orifice geometry. The division of the flowfield into these regions may be more clearly visualized by referring to the schematic diagram in Fig. 1.

Maximum Velocity Decay

Of primary concern in studies of the present type is the decay of the maximum mean velocity with X, the streamwise coordinate. The maximum mean velocity in a three-dimensional wall jet does not occur necessarily on the symmetry axis (here the X axis) in the CD region. This is the phenomenon described as velocity irregularities introduced, for the wall jet flowfields, by Viets and Sforza.[1] This feature of three-dimensional wall jets will be discussed at greater length in a subsequent section of this report. For the moment it is only necessary to state that in the present report the term mean maximum velocity denotes the maximum mean velocity in a profile taken normal to the plate along the X axis in the plane $Y = 0$.

In the case of "two-dimensional" wall jets, the decay of maximum velocity has been reported by Sigalla[3] and Bradshaw and Gee[5] to be roughly proportional to $X^{-0.5}$. However, the results of the present investigation indicates that the definition of a two-dimensional region with the flowfield generated by a finite slot may be quite arbitrary. Indeed, it is not clear, in view of the velocity irregularities observed in the transverse profiles, what relationship exists between the results obtained from slot jets and the truly two-dimensional counterpart.

For the slender orifices of eccentricity e = 0.025 and e = 0.05 the maximum velocity in the CD region decays as $X^{-.41}$ and $X^{-.44}$, respectively. These results are in fair agreement with those of Sigalla[3] and Bradshaw and Gee.[5] In the RD region $U_m \sim X^{-1.15}$ for both orifices, indicating a radial type wall jet decay as found by Bakke,[4] his result being $U_m \sim X^{-1.12\pm0.03}$. The results for these cases are shown in Figs. 2a and 2b.

For the orifice of eccentricity e = 0.10 the maximum velocity decay is shown in Fig. 2c and is found to be proportional to $X^{-0.16}$ in the CD region and $X^{-1.09}$ in the RD region. Again the decay in the RD region is equal to that found for the radial wall jet.

For the square orifice (e = 1.0) there is a direct transition to a radial wall jet decay. This is shown in Fig. 2d, where the maximum velocity is seen to decay as $X^{-1.14}$.

The flowfield for an e = 10.0 orifice (i.e., the e = 0.10 orifice with its narrow side tangent to the plate) was investigated primarily out of curiosity since it fits neither the slender nor the bluff orifice description. The results for this case are not considered here; see Ref. 2 for further details.

Velocity Half-Widths

Two velocity half-widths appear in the present problem: one normal to the plate ($Z_{1/2}$), the other parallel to it ($Y_{1/2}$). These quantities are described in Fig. 1.

Figures 3a and b present the transverse half-width growths for the e = 0.025 and e = 0.05 orifice. Here it is seen that $Y_{1/2}$ is a constant in the near region of the flowfield and then begins to increase as the flow develops further.

For the orifices e = 0.10 and e = 1.0, a different type of pattern is observed. Figures 3c and d show that for both orifices $Y_{1/2}$ first decreases, crosses over $Z_{1/2}$, and then rapidly increases. Here, the transverse half-width is said to "neck-down" in the CD region.

From Figs. 4a and b, which are composites of the half-width growths for the slender and bluff orifices, two important conclusions can be deduced. First, the $Z_{1/2}$ (normal half-width) growths in the X direction are essentially the same for all the conventional wall jets tested. Secondly, far downstream the $Y_{1/2}$ (transverse half-width) growth becomes oblivious of the orifice geometry, since again the growth rate becomes identical for all the flows. It may be noted here that the normal and transverse growth rates are not equal; the spreading across the plate is the more rapid far downstream.

Similarity of Velocity Profiles

For each one of the wall jets tested the flow region was investigated for flow similarity. Glauert[16] has obtained theoretical descriptions for wall jets for cases in which similarity exists for both two-dimensional and radial wall jets.

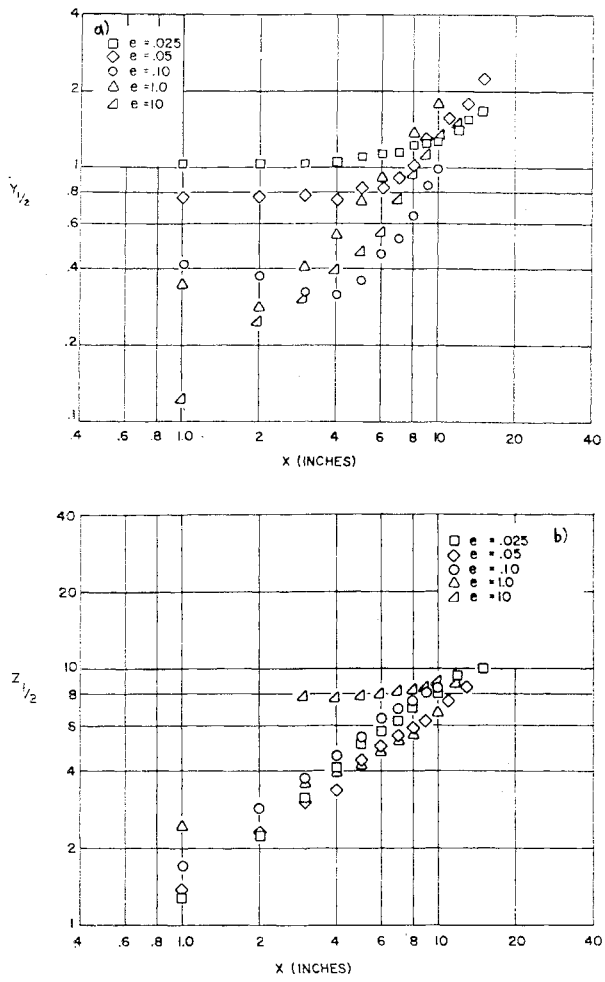

Fig. 4 Composite of half-width growths for all wall jets tested: a) $Y_{1/2}$ vs X, b) $Z_{1/2}$ vs X.

Here, for the three-dimensional wall jet flows investigated, similarity was observed in both the CD and RD regions. These results have been compared with Glauert's predictions.

Centerline similarity profiles normal to the plate for the $e = 0.025$, $e = 0.05$, $e = 0.10$, and $e = 1.0$ orifices are presented in Ref. 2. In the characteristic decay regions these profiles agree quite well with Glauert's two-dimensional profiles ($\alpha = 1.25$). Those in the radial decay region are in very good agreement with his results for the radial wall jet profile ($\alpha = 1.3$). It must be noted that the differences in the profiles described by the two different values of α are not great. Representative similarity profiles, for the $e = 0.10$ orifice, are shown in Fig. 5.

An extensive study was performed on the $e = 0.10$ orifice wall jet to determine whether or not streamwise profile similarity exists off the $Y = 0$ plane. The experiments indicated that normal profile similarity exists up to $\bar{Y} = 2.0$ off the centerline, but deteriorates at $\bar{Y} = 2.5$, and beyond. Results of this study appear in Ref. 2.

Similarity profiles in the transverse direction for the RD region are also presented for all the orifices in Ref. 2. In Fig. 5, typical profiles for the $e = 0.10$ orifices at $Z = Z_m$ and at an arbitrarily picked height of $Z = 0.06$ in. from the plate are depicted. It is apparent that similarity is achieved at reasonable distances from the orifice. For all the orifices except $e = 10.0$ the similarity profiles are approximately the same.

Velocity Irregularities

Nonuniformities in the velocity distribution in planes parallel to the plate have been reported by a number of investigators studying the flowfield of so-called two-dimensional wall jets. In most cases, only brief mention is made of these irregularities, i.e., Sigalla,[3] Schwarz and Cosart,[8] Bradshaw and Gee,[5] Kruka and Eskinazi[9]; by others, such as Nishimura,[17] data has been presented, and in Viets and Sforza[1] data is presented and an explanation is offered.

Here, as shown for the three-dimensional freejet by Sforza, Steiger, and Trentacoste,[14] and Trentacoste and Sforza,[15] the velocity irregularities appear in the near field (CD region). In the three-dimensional freejet the velocity irregularities are believed to be caused by the induced velocity distribution connected with a system of vortex rings surrounding the jet.

The wall jet flowfield is generally considered to be split into two parts as one proceeds in a direction normal to the plate. That is, an inner portion which exhibits the characteristics of a boundary-layer flow over a surface and an outer portion which exhibits the characteristics of a freejet type flowfield. A superstructure of horseshoe vortices surrounding this outer region (see Fig. 6a) would induce velocities in the remainder of the flow which can account for this irregular behavior in the velocity distribution parallel to the plate. As the flow proceeds downstream in X, these

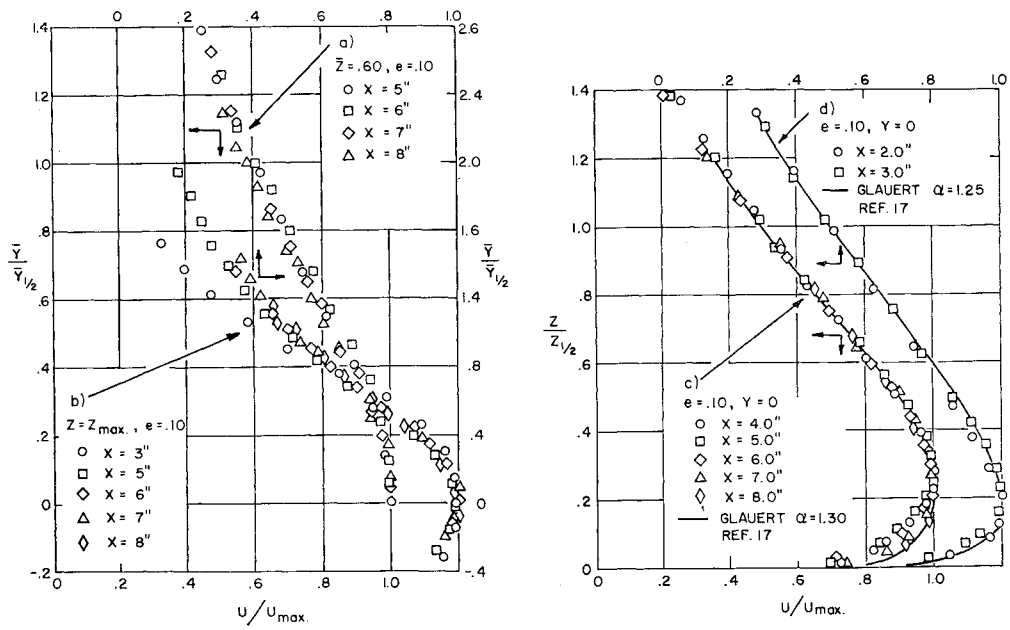

Fig. 5 Velocity profiles in similarity form for $e = 0.10$ wall jet. Spanwise profiles at: a) $\bar{Z} = 0.60$ and b) $\bar{Z} = \bar{Z}_{max}$. Normal profiles along $Y = 0$ for c) RD region, d) CD region.

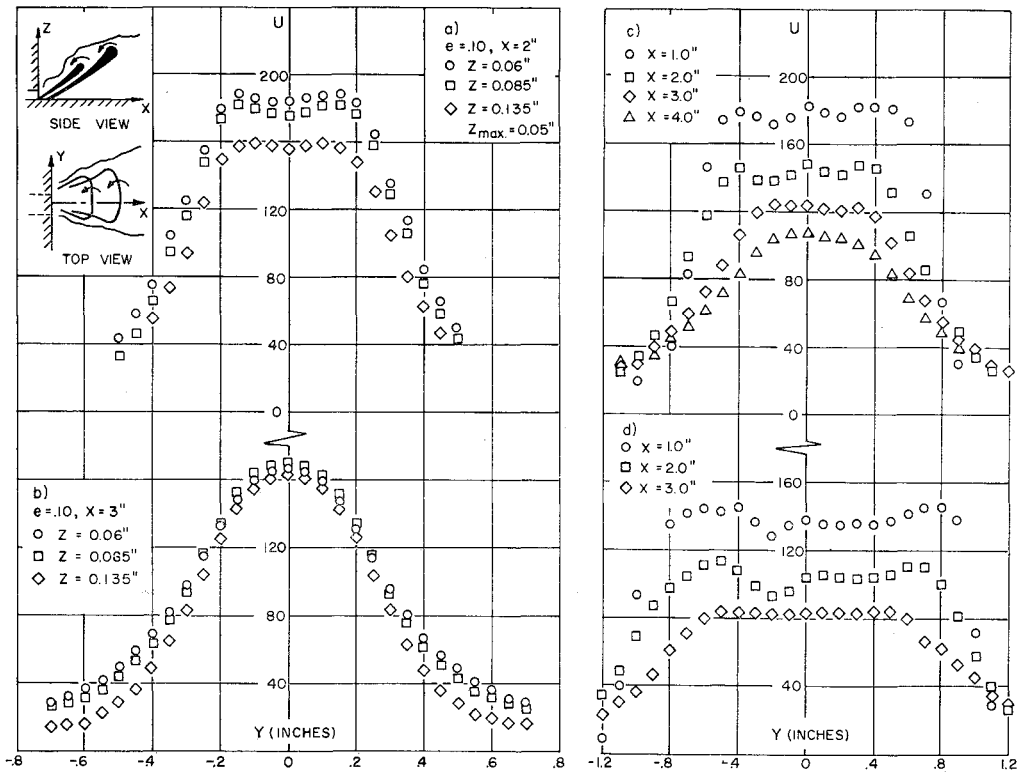

Fig. 6 Spanwise velocity profiles for: a) $e = 0.10$ wall jet at $X = 2$ in., b) $e = 0.10$ wall jet at $X = 3$ in., c) $e = 0.05$ wall jet for various X, d) $e = 0.025$ wall jet for various X. Inset shows schematic view of horseshoe vortices (dark lines) in wall jet near field.

vortices merge and diffuse (as in the case of the freejet), thus reducing the effectiveness of their induced velocity field.

Far downstream in the RD region, no trace of this irregular behavior in the velocity distribution parallel to the plate can be observed, thus indicating that complete diffusion of the surrounding vortices has taken place.

Some representative results of these irregularities from the present investigation for the $e = 0.10$ orifice at different heights above the plate are presented in Fig. 6. They are present at $X = 2$ in. (Fig. 6a) but cease to exist at $X = 3$ in. as is shown in Fig. 6b. Results for the orifices $e = 0.05$ and $e = 0.025$ are presented in Figs. 6c and d, respectively. These transverse velocity profiles were taken at the height where the velocity in the profile normal to the plate was a maximum. Here again, as for the $e = 0.10$ orifice, the velocity irregularities decay with the streamwise coordinate X.

Extent of Two-Coordinate Flow

For the more slender jets tested, i.e., $e = 0.025$ and 0.05, there appears to be a region of two-coordinate flow. That is, the irregularities are no longer discernible and a relatively flat velocity profile in the spanwise direction is observed, as in Figs. 6c and d. Furthermore, this occurs within the CD region of the jet. One would be tempted to suggest that this restricted region of the flowfield is quasi-two-dimensional. There are three objections to this conclusion.

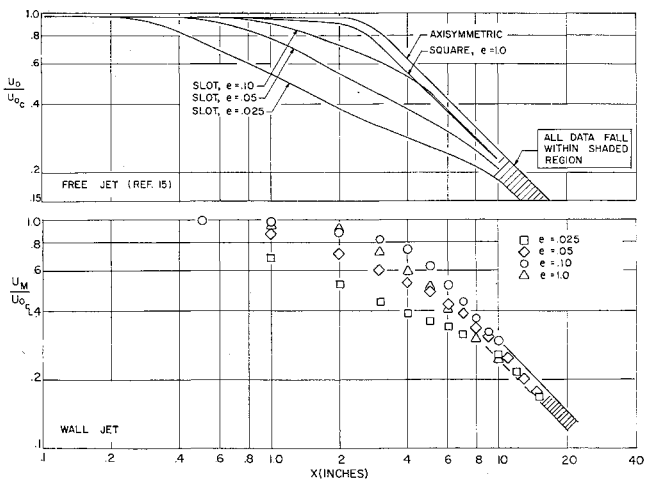

Fig. 7 Comparison of maximum velocity decay for freejet and wall jet.

First, the magnitude of the nonuniformities generally increases as Z increases beyond Z_{max}. A maximum is achieved and then the magnitude of the velocity irregularities decreases as Z is increased further. Therefore, there may exist irregularities in the flowfield at $Z > Z_{max}$ even though there is a small extent of uniform velocity in the spanwise direction at $Z = Z_{max}$.

Secondly, the contours of constant velocity (Ref. 2, Fig. 38) indicate that the flowfield is somewhat oval in cross section. Therefore, the spanwise extent of uniform flow is quite small near the plate, increases as Z increases, and then diminishes as Z increases beyond Z_{max}. In turn, the spanwise extent of two-coordinate flow throughout the full profiles normal to the plate is much smaller than indicated by the flat portion of the velocity profiles at the Z_{max} station.

Finally, and most importantly, the stations at which this uniformity of maximum velocity across a small portion of the flowfield in the Y direction appears is immediately preceded by the region of large velocity nonuniformities. This phenomenon has been suggested to be due to the presence of a strong, concentrated vortex superstructure, and its attendant induced velocity field. Therefore, it appears that the vortex structure, which is dependent upon the orifice geometry and is highly three-dimensional in character, has strongly influenced the flowfield prior to its attaining a small measure of uniformity. This indicates that the concentrated vorticity has been effectively dissipated by turbulent mixing and the more regular profile is a result of this dissipation. The resulting smooth profile is achieved by turbulent diffusion and its subsequent decay is diffusive in character, i.e., smooth, with a rounding-out of the profiles.

Comparison of Wall and Freejets

Three-dimensional wall jets have many features in common with those of their freejet counterparts. Both flow-

fields may be conveniently divided into three distinct regions based on the streamwise decay of the maximum velocity. Each region in the wall jet flowfield is analogous to its freejet counterpart: both have 1) potential core regions, 2) characteristic decay regions in which the orifice geometry has an important effect, and 3) an asymptotic decay region where the flow behaves as if it were generated by a point source.

Indeed, the maximum velocity decay for both freejets and wall jets are very similar in appearance as shown in Fig. 7. In both cases the maximum velocity distribution in the CD region is clearly dependent on the orifice geometry. However, as the flow proceeds further downstream, all the decay rates approach the appropriate asymptotic value: $u_m \sim X^{-1}$ and $X^{-1.1}$ for the freejets and wall jets, respectively.

Further evidence of the similarities between wall jets and freejets, with respect to the streamwise decay of maximum mean velocity, is depicted in Fig. 8. Here the exponent N, which describes the decay of maximum velocity according to the relation $u_m \sim X^{-N}$, is plotted for various values of e for both wall jets and freejets within the CD region. It is evident that the variation of N for increasing e is not monotonic for both types of flowfields.

Trentacoste and Sforza[15] found that the freejet with $e = 0.10$ had superior mass entrainment properties compared to the axisymmetric jet; the former also displayed the slowest decay rate of maximum velocity. Other investigations[18,19] indicate that optimum mass entrainment is achieved by freejets with $0.083 > e > 0.125$; the $e = 0.10$ jet falls in this range. It may develop that a similar result will transpire for the wall jet flowfield, i.e., that wall jets generated by orifices with an eccentricity $e \simeq 0.10$ have optimum mass entrainment characteristics. Clearly, this would be of great importance in connection with slot-jet injection systems.

It appears then that the effect of the wall on maximum velocity decay is not very pronounced. However, its influence on the streamwise growth of the wall jet is appreciable and readily apparent. In the case of the freejet, Trentacoste and Sforza[15] observed that freejets generated by slender orifices possess similar half-width growths. That is, all half-width data in both principal planes may be reduced to a single plot for all regions of the flow by utilizing a growth parameter based on the eccentricity of the orifice.

In the case of the wall jet it has been shown in Fig. 4b that the half-width growth normal to the plate ($Z_{1/2}$) is practically equivalent for all conventional orifices tested. A perusal of Fig. 4a shows that in the CD region the $e = 0.025$ and 0.05 jets have transverse half-widths ($Y_{1/2}$) which are monotonic, whereas those in the $e = 0.10$ and 1.0 jets are not monotonic. It is clear that the presence of the wall inhibits

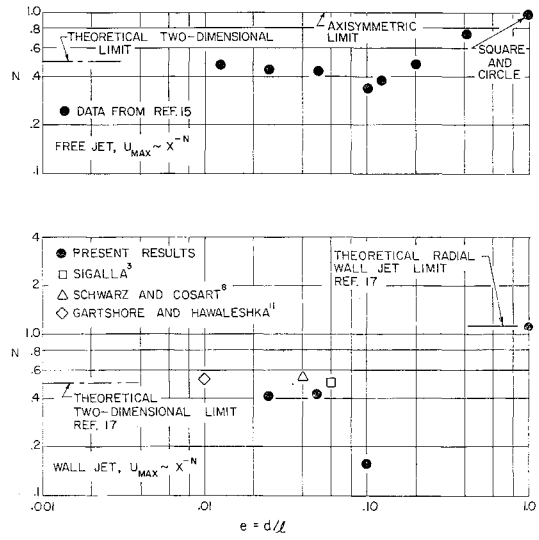

Fig. 8 Exponent (N) of maximum velocity decay for freejets and wall jets within CD region.

the necking-down of the more slender wall jets which had been observed in the freejet flowfields.[15]

Far downstream all the wall jets spread transversely at about the same rate. It may be pointed out that this spreading occurs at a faster rate than in the freejet. Therefore, it appears that the wall, which constrains the flow to the region $Z > 0$, encourages spillage in the transverse direction. This effect serves to keep the normal growth in the wall jet smaller than that in the freejet and the transverse growth larger. It is noted that, ultimately, in the far field all the wall jets have about equal spread over the plate in the transverse direction.

Surface Friction

Based on the observations reported herein, it is possible to indicate the centerline decay of the skin-friction coefficient for the three-dimensional wall jet. Consider the usual three-dimensional boundary-layer equations in the present case of the wall jet where the effect of pressure gradient is neglected in this ad hoc analysis. The continuity and X momentum equations may be combined to yield

$$(u^2)_X + (uv)_Y + (uw)_Z = (1/\rho)[(\tau_{xy})_Y + (\tau_{xz})_Z] \quad (1)$$

which, when integrated over the area of the half-space

Table 1 Compilation of half-width growths and maximum mean velocity decay for wall jets of various geometries

Type of flowfield	Investigators	Streamwise variation of half-width growth: Normal to plate ($Z_{1/2}$)	Streamwise variation of half-width growth: Spanwise ($Y_{1/2}$)	Axial decay of maximum mean velocity (u_0)
"Two-dimensional" wall jet	Sigalla[3]	$X^{1.0}$	...	$X^{-0.50}$
	Bradshaw & Gee[5]	$X^{0.91}$	...	$X^{-0.53}$
	Schwarz & Cosart[8]	$X^{1.0}$	...	$X^{-0.55}$
Radial wall jet	Bakke[4]	$X^{0.94}$	...	$X^{-1.12}$
	Poreh et al.[6]	$X^{0.9}$	...	$X^{-1.1}$
Three-dimensional wall jet	Present results	$X^{0.78\pm0.07}$ (for all conventional orifices tested, in both CD & RD regions)		CD region: $e = 0.025: X^{-0.41}$; $e = 0.05: X^{-0.43}$; $e = 0.10: X^{-0.16}$. RD region: $X^{-1.1}$ (all conventional orifices tested)

Table 2 Compilation of centerline skin-friction coefficient decay for wall jets of various geometries

Flowfield	Investigators	Streamwise variation of skin-friction coefficient: measured values	Streamwise variation of skin-friction coefficient; calculated from Eq. (6)	Variation of skin-friction coefficient with Reynolds number
"Two-dimensional" wall jet	Sigalla[3]	$X^{-0.125}$	constant	constant
	Bradshaw & Gee[5]	$X^{-0.069}$	$X^{-0.09}$	$Re_m^{-0.24}$
	Schwarz & Cosart[8]	$X^{-0.111}$	constant	constant
Radial wall jet	Bakke[4]	...	$X^{-0.06}$	$Re_m^{0.33}$
	Poreh et al.[6]	$X^{-0.10}$	$X^{-0.10}$	$Re_m^{0.50}$
Three-dimensional wall jet	Present results	...	$X^{-0.22\pm0.07}$ (all conventional orifices tested, in both CD & RD regions)	CD Region $e = 0.025 : Re_m^{-0.59}$ $e = 0.05 : Re_m^{-0.63}$ $e = 0.10 : Re_m^{-0.36}$ RD Region $Re_m^{0.69\pm0.09}$ (all conventional orifices tested)

bounded by the plate at $Z = 0$, yields

$$\int_{-\infty}^{+\infty} \int_{0}^{\infty} (u^2)_X dY dZ = -\int_{-\infty}^{+\infty} \left(\frac{\tau_{xz}}{\rho}\right) \tag{2}$$

To arrive at this point the following assumptions have been made: a) no slip at the wall, b) quiescent ambient far from the plate centerline, and c) shear symmetry in the XY plane.

By suitable nondimensionalization of variables this momentum integral relation may be recast as follows:

$$d\theta/dx \sim Y_{1/2}\tau_{xz,0} \tag{3}$$

for velocity field similarity, where

$$\theta = u_m{}^2 Y_{1/2} Z_{1/2} \sim X^{-m} \tag{4}$$

and

$$\tau_{xz,0} = \tau_{xz}(X,0,0)$$

Here we have assumed that the shear distribution in the y direction is similar, i.e. that

$$\tau_{xz}/\tau_{xz,0} = \tau(y/y_{1/2})$$

Since θ clearly has some power law variation we write

$$d\theta/dX = -m\theta/X \sim y_{1/2}\tau_{xz,0}$$

or

$$\tau_{xz,0} \sim u_m{}^2 Z_{1/2}/X \tag{5}$$

This may be expressed as the centerline value of the skin-friction coefficient

$$C_{f,0} = \tau_{xz,0}/\tfrac{1}{2}\rho u_m{}^2 \sim Z_{1/2}/X \sim X^r \tag{6a}$$

or

$$C_{f,0} \sim (u_m Z_m/\nu)^p = (Re,m)^p \tag{6b}$$

Equation (6) is the skin-friction coefficient at the wall and along the centerline of the flow for a wall jet having shear similarity. Tables 1 and 2 compare C_{fo}, the $Z_{1/2}$ half-width growth, and the maximum velocity decay for the 2-D, radial, and 3-D wall jets. The streamwise dependence of the skin-friction coefficient is calculated from Eq. (6), using the data of past investigators and compared with their result.

References

[1] Viets, H. and Sforza, P. M., "An Experimental Investigation of a Turbulent, Incompressible, Three-Dimensional Wall Jet," PIBAL Rept. 968, AFOSR 66-0888, April 1966, Polytechnic Institute of Brooklyn, Farmingdale, N. Y.

[2] Sforza, P. M. and Herbst, G., "A Study of Three-Dimensional, Incompressible Wall Jets," PIBAL Report 1022, AFOSR 67-2580, Oct. 1967, Polytechnic Institute of Brooklyn, Farmingdale, N. Y.

[3] Sigalla, A., "Measurements of Skin Friction in a Plane Turbulent Wall Jet," *Journal of the Royal Aeronautical Society*, Vol. 62, 1958, p. 873.

[4] Bakke, P., "An Experimental Investigation of a Wall Jet," *Journal of Fluid Mechanics*, Vol. 2, 1957, p. 467.

[5] Bradshaw, P. and Gee, M. T., "Turbulent Wall Jets With and Without an External Stream," R & M 3252, 1962, Aeronautical Research Council.

[6] Poreh, M., Tsuei, Y. G., and Cermak, J. E., "Investigation of a Turbulent Radial Wall Jet," *Transactions of the ASME, Journal of Applied Mechanics*, June 1967, pp. 457–463.

[7] Sawyer, R. E., "The Flow Due to a Two-Dimensional Jet Issuing Parallel to a Flat Plate," *Journal of Fluid Mechanics*, Vol. 9, Pt. 4, 1961.

[8] Schwarz, W. H. and Cosart, W. P., "The Two-Dimensional Turbulent Wall Jet," *Journal of Fluid Mechanics*, Vol. 10, Pt. 4, June 1961.

[9] Kruka, V. and Eskinazi, S., "The Wall Jet in a Moving Stream," *Journal of Fluid Mechanics*, Vol. 20, Pt. 4, 1964, pp. 555–579.

[10] Gartshore, I. S., "Jets and Wall Jets in Uniform Streaming Flow," Rept. 64-4, May 1964, Mechanical Engineering Labs., McGill Univ., Canada.

[11] Gartshore, I. S. and Hawaleshka, O., "The Design of a Two-Dimensional Blowing Slot and Its Application to a Turbulent Wall Jet in Still Air," Rept. 64-5, June 1967, Mechanical Engineering Labs., McGill Univ., Canada.

[12] Gartshore, I. S., "The Streamwise Development of Certain Two-Dimensional Turbulent Shear Flows," Rept. 64-3, April 1965, Mechanical Engineering Labs., McGill Univ., Canada.

[13] Rajaratnam, N. and Subramanya, K., "An Annotated Bibliography on Wall Jets," July 1967, Dept. of Civil Engineering, Univ. of Alberta, Canada.

[14] Sforza, P. M., Steiger, M. H., and Trentacoste, N., "Studies on Three-Dimensional Viscous Jets," *AIAA Journal*, Vol. 4, No. 5, May 1966, pp. 800–806.

[15] Trentacoste, N. and Sforza, P. M., "An Experimental Investigation of Three-Dimensional Free Mixing in Incompressible Turbulent Free Jets," PIBAL Rept. 871, AFOSR 66-0651, March 1966, Polytechnic Institute of Brooklyn, Farmingdale, N. Y.; also "Further Experimental Results for Three-Dimensional Free Jets," *AIAA Journal*, Vol. 5, No. 5, May 1967, pp. 885–891.

[16] Glauert, M. B., "The Wall Jet," *Journal of Fluid Mechanics*, Vol. 1, 1956, p. 625.

[17] Nishimura, Y., "Application of a Jet Pump and Coanda Surface to Ventilation of a Highway Tunnel," UTIAS TN-82, Feb. 1965, Univ. of Toronto Institute for Aerospace Studies, Canada.

[18] Tuve, G. L., Priester, G. B., and Wright, D. K., "Entrainment and Jet-Pump Action of Air Streams," *Journal of Heating and Ventilation*, Vol. 48, No. 1204, 1942.

[19] Manganiello, E. J. and Bogatsky, D., "An Experimental Investigation of Rectangular Exhaust Gas Ejectors Applicable for Engine Cooling," WRE-224, May 1944, NASA.

FEBRUARY 1970 AIAA JOURNAL VOL. 8, NO. 2

Blowing from a Porous Cone with an Embedded Shock Wave

GEORGE EMANUEL*
Aerospace Corporation, El Segundo, Calif.

Massive blowing from a porous cone in a supersonic flow is considered under the assumptions of inviscid, conical flow. The injection is assumed to be uniform, normal, and supersonic. This last assumption requires a straight shock wave in the injected flowfield. The numerically obtained solutions have two noteworthy features. First, the contact surface angle relative to the cone's axis decreases sharply when the embedded shock wave moves off the body. Second, it is possible to have a completely supersonic flow from the outer shock wave to the body, so that any upstream effect due to the presence of the cone's base is eliminated. Detailed solutions are presented and a model for the porous wall is used to relate the position of the embedded shock wave to freestream and plenum conditions.

Nomenclature

C_{pc} = contact surface pressure coefficient
M = Mach number, $q/(\gamma p \rho^{-1})^{1/2}$
$M_\perp$ = $M \sin(\phi - \eta)$
$\bar{M}_b$ = maximum value for M_b [see Eq. (8)]
p = pressure
P = p/p_b
q = flow velocity
R = universal gas constant
T = temperature
β = porosity
γ = (constant) ratio of specific heats
η = ray angle relative to the body
θ_b = body half angle
ρ = density
ϕ = flow inclination angle relative to the body
χ = blowing parameter [see Eq. (5)]

Subscripts

b = conditions on body surface
c = conditions at contact surface
s = embedded shock wave
0 = plenum conditions
1 = conditions ahead of the embedded shock wave
2 = conditions behind the embedded shock wave
∞ = freestream conditions

I. Introduction

IN a previous Paper,[1] uniform, normal, subsonic injection of a perfect gas from a porous cone in a supersonic flow was examined in detail. (This type of flow was first proposed by Aroesty and Davis.[2]) The basic assumption was that the solution for the injected flowfield is inviscid and conical. This results in a straight contact surface and a Taylor-Maccoll flow exterior to the contact surface. Another assumption was that the injected flowfield is continuous, i.e., shock free. In this case, supersonic normal injection is not possible, because the injected flow curves in an upstream direction.

The idea of supersonic injection from a porous wall is a novel one. It was first predicted theoretically[3] for the flow downstream of a porous plate located transversely in a duct, and it was subsequently verified experimentally by Shreeve[4]. Supersonic injection (with an embedded shock wave) has also recently been observed[5] in the injected flow from a porous plate.

To remove the aforementioned difficulty with supersonic injection, it is necessary to have a shock wave in the injected flow. With a straight embedded shock, supersonic normal injection is indeed possible. This work extends the inviscid conical theory of Ref. 1 to include this situation.

A number of objections have been raised against the conical flow assumption. It is appropriate, therefore, to examine some of these objections. The first[6] was that the pressure at the vertex of the cone is multivalued both inside and outside the contact surface. Furthermore, since the flow inside the contact surface in Ref. 1 and in some of the cases treated here is subsonic, such a singularity in pressure is claimed to be not admissible.[6] However, this type of flow does occur, as demonstrated by the existence of subsonic Taylor-Maccoll flow.[7]

A second objection is that the upstream effect, caused by the base of a finite cone, violates the conical assumption. When some or all of the injected flow, or the outer Taylor-Maccoll flow, is subsonic this objection is only partially correct. In this situation the conical solution should hold close to the cone's tip, as it is known to hold for ordinary subsonic (or transonic) Taylor-Maccoll flow. With supersonic injection, however, it is possible to have a completely supersonic flow from the outer shock to the body, so that the upstream effect is eliminated. This paper discusses some of the conditions under which this type of flow might be attained.

Another objection is that the analysis in Ref. 1 and in this work yields contact surface angles larger than those found by Hartunian and Spencer.[8] In their experiments, the contact surface was located by the emission of a chemiluminescent reaction; the location of the freestream shock wave was not determined. These experiments, however, failed to satisfy

Received November 15, 1968; revision received July 31, 1969. This work was performed under Air Force Contract F04701-68-C-0200. The author acknowledges with pleasure the suggestion by P. A. Libby of the University of California at La Jolla that he study supersonic injected flow, the helpful discussions with M. Epstein of Aerospace Corporation, and finally the competent assistance of the Mathematics and Computation Center of Aerospace Corporation in obtaining the numerical results.

* Manager, Theoretical Gas Dynamics Section, Aerodynamics and Propulsion Research Laboratory. Member AIAA.